Size-dependent free vibration analysis of multidirectional functionally graded nanobeams via a nonlocal strain gradient theory

Mohamed Guerroudj[1] · Ahmed Drai[1,2] · Ahmed Amine Daikh[3,4] ·
Mohammed Sid Ahmed Houari[4] · Benaoumeur Aour[1] ·
Mohamed A. Eltaher[5,6] · Mohamed-Ouejdi Belarbi[7,8]

Abstract

The free vibration behavior of a new advanced functionally graded (FG) nanobeam is presented in this work using the recently proposed nonlocal higher-order shear deformation theory. In the present theory, the stress tensor can satisfy the parabolic variation of the shear stress distribution throughout the thickness direction and also fulfill the requirement that the shear stress on the top and bottom surfaces of the FG nanobeam is zero. Two common types of FG structures, namely, FG hardcore and FG softcore, are considered here for analysis with three schemes. The material properties of the FG nanobeam are assumed to vary continuously in both the longitudinal and transversal directions according to a combined simple power-law distribution in terms of the volume fractions of the constituents. The governing equations of the FG nanobeam with

✉ Mohamed-Ouejdi Belarbi
  mo.belarbi@univ-biskra.dz

1   Laboratory of Applied Biomechanics and Biomaterials (LABAB), ENP Oran, BP1523 El Mnaour, 31000 Oran, Algeria

2   Department of Mechanical Engineering, University of Mustapha Stambouli, Mascara, Algeria

3   Artificial Intelligence Laboratory for Mechanical and Civil Structures, and Soil, University Centre of Naama, P.O. Box 66, 45000 Naama, Algeria

4   Laboratoire d'Etude des Structures et de Mécanique des Matériaux, Département de Génie Civil, Faculté des Sciences et de la Technologie, Université Mustapha Stambouli, B.P. 305, 29000 Mascara, Algeria

5   Mechanical Design and Production Department, Faculty of Engineering, Zagazig University, P.O. Box 44519, Zagazig, Egypt

6   Mechanical Engineering Department, Faculty of Engineering, King Abdulaziz University, P.O. Box 80204, Jidda, Saudi Arabia

7   Laboratoire de Recherche en Génie Civil, LRGC, Université de Biskra, B.P. 145, 07000 Biskra, Algeria

8   Department of Civil Engineering, Lebanese American University, Byblos, Lebanon

simply supported boundary conditions are derived using the proposed higher-order shear deformation plate theory. The nonlocal strain gradient theory is employed to capture the microstructure-dependent effect. The influence of the structural geometry, the gradient index, and the nonlocal and length scale parameters on the vibration frequency is investigated. Finally, many new results are also reported in the current study, which will serve as a benchmark for future research.

Keywords Free vibration · Higher-order shear deformation theory · Multidirectional FG beam · Nonlocal strain gradient theory

1 Introduction

Functionally graded materials (FGMs) are advanced composite materials characterized by microscopically varying material properties throughout their structure, resulting in a continuous transition from one surface to another. These materials exhibit a spatial gradient in macroscopic mechanical strength and thermal conductivity. Nowadays, the use of functionally graded structures has become increasingly prevalent in various engineering sectors such as aerospace, aircraft, automotive, and others. One of the significant advantages of functionally graded materials over traditional composites is their ability to overcome interface challenges commonly encountered in conventional materials.

In recent years, nanostructures such as nanorods, nanobeams, and nanoplates have attracted considerable attention for their exceptional mechanical, thermal, chemical, and electronic properties [1, 2]. These structures are increasingly used in micro/nano electromechanical systems (MEMS/NEMS) and nano actuators, leading to a growing interest in modeling micro and nanoscale structures. Size effects at the nanoscale are widely acknowledged to be significant, prompting further development of design and analysis methods to accurately simulate their impact on mechanical responses. As a result, improved non-classical continuum-based elasticity theories with scale parameters have been developed to provide a practical framework for considering size effects without excessive computational costs.

One of the most common enhanced continuum-based theories of elasticity is Eringen's strain-driven nonlocal model [3, 4]. This model assumes that stress at any point is represented by the convolution integral of elastic strain at each point of the medium and a decaying kernel function, introducing a nonlocal constant to evaluate the intensity of long-range interactions in the medium. To circumvent the difficulties inherent in solving the corresponding integro-differential equations found in many structural problems [5, 6], the subsequent differential law is commonly used to replace the original nonlocal integral deformation. Interested readers are encouraged to consult the review literature [7–9] and the articles cited therein.

Numerous studies have been conducted to investigate the mechanical responses of nanostructures using these theories. Researchers have analyzed Euler–Bernoulli nanobeams using nonlocal elasticity theory [10], studied the vibration behavior of functionally graded nanobeams in thermal environments [11], explored the surface effects on deformations of magneto–electro-elastic beams [12], and investigated the

vibration and thermal buckling of nonlocal functionally graded nanobeams [13], among other studies. Nonlocal beam theories have been employed to examine the mechanical behavior of micro and nanostructures [14, 15], and comprehensive reviews have been conducted on the benefits and drawbacks of nonlocal theory [8]. Furthermore, exact solutions for bending, buckling, and free vibration of functionally graded carbon nanotube-reinforced composite nanobeams have been proposed based on nonlocal theory [16], and static bending and buckling of functionally graded nanoscale beams have been studied using nonlocal Timoshenko beam models [17]. A study conducted by Ebrahimi and Barati [18] focused on the thermal vibration behavior of functionally graded (FG) nanobeams subjected to different types of thermomechanical loading, including uniform, linear, and nonlinear temperature rise. They utilized a two-parameter elastic foundation based on the third-order shear deformation beam theory and incorporated the nonlocal size-dependent effect to analyze the static and dynamic behavior of isotropic and functionally graded beams at a small scale.

A series of papers by Barretta and co-workers [19, 20] indicated that when adopting the classical Helmholtz-type kernel, Eringen's model becomes ill-posed in formulating mechanical problems of bounded structures. This occurs due to the constitutive boundary conditions inherent in the differentiation process of the strain-driven integral model being satisfied only by default in problems involving unbounded domains, for example, in problems concerning dislocation and wave propagation studied by Eringen. However, the inherent constitutive boundary conditions for bounded structures may be incompatible with the equilibrium requirements of the corresponding problems, leading to inconsistent results. For instance, perhaps the most well-known inconsistency is the conclusion that raising the nonlocal length scale parameter shows a softening effect for all beam boundary edges except for cantilever nanobeams under point loading conditions [21, 22]. This ill-posedness of Eringen's strain-driven model is also demonstrated in many recent papers [23–26].

Yang et al. [27] proposed the modified couple stress theory, which considers a symmetric couple stress tensor and includes only one additional parameter. However, the modified couple stress theory can be regarded as a special case of the modified strain gradient theory. Recent theoretical works have focused on the mechanical and dynamic behaviors of small-scaled structures using strain gradient theory and modified couple stress theory [28–32]. These gradient elasticity models have shown a stiffness enhancement effect. It is important to note that nonlocal elasticity models and strain gradient models describe distinct size-dependent mechanical and physical characteristics of small-scaled materials and structures. To investigate the effects of these two size-dependent phenomena on structural responses, researchers have developed nonlocal strain gradient models. Papargyri-Beskou et al. [33] derived the governing equation and boundary conditions for the buckling analysis of an Euler–Bernoulli beam using the variational principle based on the simple theory of gradient elasticity with surface energy. Lim et al. [34] proposed a nonlocal strain gradient theory that combines both strain gradient and nonlocal elasticity models, aiming to evaluate the impacts of nonlocal and length scale parameters on the mechanical and physical responses of size-dependent structures. This model has attracted significant attention from researchers studying small-scale structures.
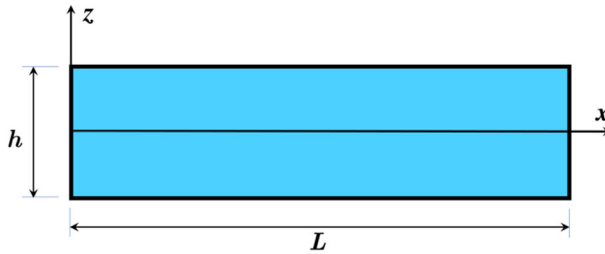
Fig. 1 FG beam geometry

Li et al. [35] investigated the free vibration analysis of nonlocal strain gradient beams made of functionally graded material. They derived a size-dependent Timoshenko beam model considering through-thickness power-law variation and found significant effects of such grading on natural frequencies and stiffness. Another study by Li et al. [36] delved into the nonlinear bending and free vibration analyses of similar beams, showing smaller nonlinear bending deflections and higher vibration frequencies compared to linear counterparts due to intrinsic stiffening effects. Özmen et al. [37] explored the thermomechanical vibration and buckling response of nonlocal strain gradient porous FG nanobeams in magnetic and thermal fields. They demonstrated the effects of nonlocal differential and strain gradient elasticities on softening and stiffness enhancements. These studies contribute to understanding the complex behavior of nanobeams under various conditions, aiding in the design of micro/nano electromechanical systems. Other recent studies have focused on specific applications, such as Daikh et al. [38] conducting a comprehensive study on the static deflection and buckling stability of axially loaded FG carbon-nanotube-reinforced composite (FGCNTRC) plates with temperature-dependent material properties.

The objective of this paper is to investigate the free vibration response of a novel advanced functionally graded nanobeam. Based on the nonlocal theory, a size-dependent hyperbolic shear deformation beam model is developed for the vibration behavior of FG nanobeam using nonlocal theory. The most interesting feature of this theory is that it accounts for a parabolic variation of the transverse shear strains across the thickness and satisfies the zero traction boundary conditions on the top and bottom surfaces of the beam without using shear correction factors. Governing equations of FGM beam with simply supported boundary conditions are derived using new higher-order shear deformation beam theory. The nonlocal theory is employed to capture the microstructure-dependent effect. Analytical solutions for vibration are provided for simply supported beams, and the obtained results are verified by comparing them with those reported in the literature to ensure the accuracy of the present theory. The influence of structure geometry, gradient index, and nonlocal scale parameters on vibration frequency is investigated.

2 Geometrical modeling and material distribution functions

A uniform beam in the Cartesian coordinate system (x, z) with length "L" and thickness "h" is shown in Fig. 1. The beam is made of ceramic and metal. Material properties are graded continuously from surfaces to the core. The effective mechanical properties, such as Young's modulus (E), density (ρ), and Poisson's ratio (υ), can be portrayed by the law of mixture as

$$P(x, z) = P_\mathrm{m} + (P_\mathrm{c} - P_\mathrm{m})V(x, z), \tag{1}$$

where P_m and P_c are the corresponding mechanical properties of the metal and the ceramic constituents. $V(x, z)$ is the volume fraction of the ceramic phase in the x and z directions.

Functionally graded materials with coatings find applications in various industrial components like turbine blades, cutting tools, and aircraft engines. Due to the complexity of these structures, there is a demand for both analytical and numerical analysis. This paper introduces a mathematical model for multidirectional functionally graded structures, a novel contribution to the field. This analysis considers two prevalent types of FG structures: FG hardcore (HC) and FG softcore (SC), examined through three schemes: FG-A, FG-B, and FG-C (Fig. 2). The material properties of the FG nanobeam are assumed to undergo continuous variation in both longitudinal and transverse directions, following a combined simple power-law distribution as illustrated in Fig. 3.
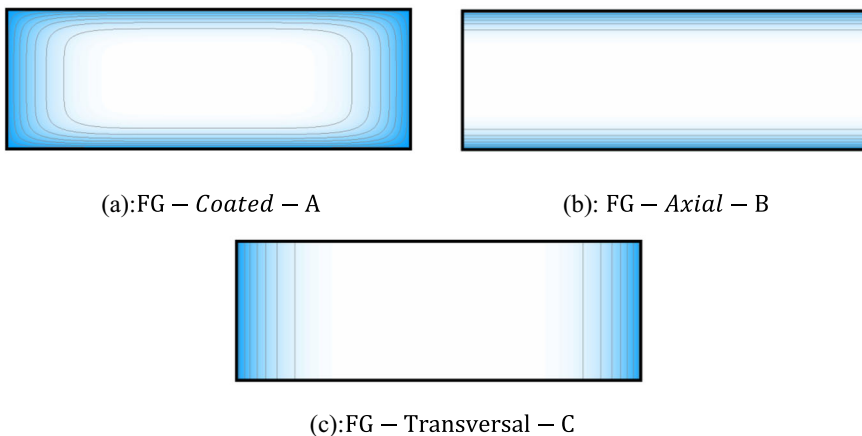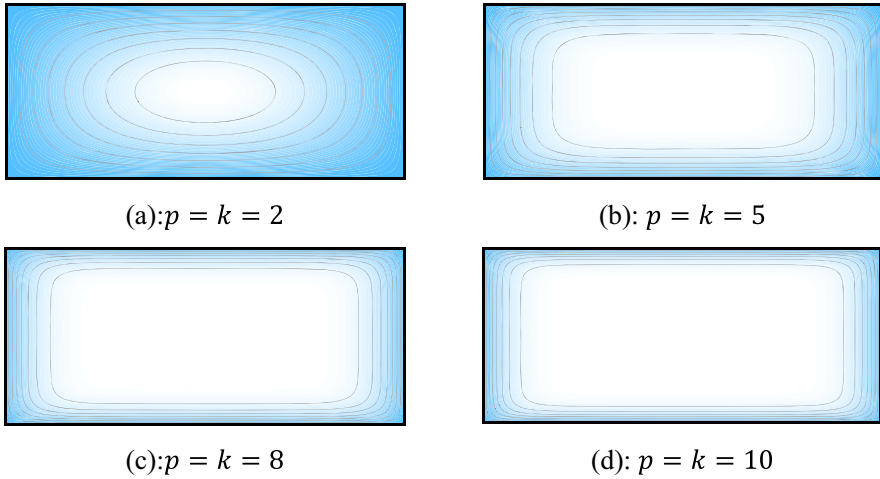

(a):FG $-$ $Coated$ $-$ A   (b): FG $-$ $Axial$ $-$ B

(c):FG $-$ Transversal $-$ C

Fig. 2 Types of FG structures

<div align="center">(a): $p = k = 2$</div>

<div align="center">(b): $p = k = 5$</div>

<div align="center">(c): $p = k = 8$</div>

<div align="center">(d): $p = k = 10$</div>

Fig. 3 Material distribution schemes

2.1 Hardcore FG beam (HC)

(a) **HC FG-A beam**

$$V_{\text{FG}-\text{A}}(x, z) = \left[\left(\frac{|2z|}{h}\right)^{p} - 1\right]\left[\left(\frac{|2x - L|}{L}\right)^{k} - 1\right]. \tag{2}$$

(b) **HC FG-B beam**

$$V_{\text{FG}-\text{B}}(z) = \left[\left(\frac{|2z|}{h}\right)^{p} - 1\right]. \tag{3}$$

(c) **HC FG-C beam**

$$V_{\text{FG}-\text{C}}(x) = \left[\left(\frac{|2x - L|}{L}\right)^{k} - 1\right]. \tag{4}$$

2.2 Soft-core FG beam (SC)

(a) **SC FG-A beam**

$$V_{\text{FG}-\text{A}}(x, z) = 1 - \left[\left(\frac{|2z|}{h}\right)^{p} - 1\right]\left[\left(\frac{|2x - L|}{L}\right)^{k} - 1\right]. \tag{5}$$

(b) **SC FG-B beam**

$$V_{FG-B}(z) = 1 - \left[\left(\frac{|2z|}{h}\right)^p - 1\right]. \tag{6}$$

(c) **SC FG-C beam**

$$V_{FG-C}(x) = 1 - \left[\left(\frac{|2x - L|}{L}\right)^k - 1\right]. \tag{7}$$

3 Kinematic equations

3.1 Displacement field

The formulation is constrained to linear elastic material behavior. The displacement field is selected under the following assumptions:

– The axial and transverse displacements are divided into bending and shear components.
– The bending component of axial displacement resembles that described by the CBT.
– The shear component of axial displacement leads to higher-order variations of shear strain, resulting in shear stress vanishing on the top and bottom surfaces of the beam.

With these assumptions, the displacement fields of various higher-order shear deformation beam theories are provided in a general form [39]:

$$u(x, z, t) = u_0 - z\frac{\partial w_0}{\partial x} + f(z)\varphi_x, \tag{8a}$$

$$w(x, z, t) = w_0, \tag{8b}$$

with,

$$f(z) = h\sinh\left(\frac{z}{h}\right) - \frac{3z^3}{2h^2}. \tag{9}$$

And

$$g(z) = f'(z). \tag{10}$$

The values u_0 and w_0 are the displacement components in the x and z directions, respectively, and φ_x is the rotation of the cross-section of the beam. The deformations associated with the displacements are

$$\varepsilon_{xx} = \varepsilon_{xx}^0 - z\varepsilon_{xx}^1 + f(z)\varepsilon_{xx}^2, \tag{11a}$$

$$\gamma_{xz} = \frac{\mathrm{d}f(z)}{\mathrm{d}z}\varphi_x. \tag{11b}$$

Therefore, we obtain the deformations in the form:

$$\varepsilon_{xx}^0 = \frac{\mathrm{d}u}{\mathrm{d}x}, \tag{12a}$$

$$\varepsilon_{xx}^2 = \frac{\mathrm{d}\varphi_x}{\mathrm{d}x}, \tag{12b}$$

$$\varepsilon_{xx}^1 = \frac{\mathrm{d}^2 w}{\mathrm{d}x^2}. \tag{12c}$$

The constitutive relations can be written as follows:

$$\left\{ \begin{matrix} \sigma_{xx} \\ \tau_{xz} \end{matrix} \right\} = \begin{bmatrix} Q_{11} & 0 \\ 0 & Q_{66} \end{bmatrix} \left\{ \begin{matrix} \varepsilon_{xx} \\ \gamma_{xz} \end{matrix} \right\}. \tag{13}$$

The stiffness coefficients are expressed as follows:

$$Q_{11} = \frac{E(z)}{1 - \upsilon^2}, \quad Q_{66} = \frac{E(z)}{2(1 + \upsilon)}. \tag{14}$$

3.2 Resulting efforts

The resultants of forces and moments can be expressed in terms of stresses in the following form:

$$\left\{ \begin{matrix} N_{xx} \\ M_{xx} \\ P_{xx} \end{matrix} \right\} = \int_{-h/2}^{h/2} \left\{ \begin{matrix} 1 \\ z \\ f(z) \end{matrix} \right\} \sigma_{xx}\mathrm{d}z, \tag{15a}$$

$$Q_{xz} = \int_{-h/2}^{h/2} \frac{\mathrm{d}f(z)}{\mathrm{d}z}\tau_{xz}\mathrm{d}z. \tag{15b}$$

We simplify the Eq. (14) to obtain

$$\left\{ \begin{matrix} N_{xx} \\ M_{xx} \\ P_{xx} \end{matrix} \right\} = \begin{bmatrix} A_{11} & B_{11} & C_{11} \\ B_{11} & D_{11} & F_{11} \\ C_{11} & F_{11} & H_{11} \end{bmatrix} \left\{ \begin{matrix} \varepsilon_{xx}^0 \\ \varepsilon_{xx}^1 \\ \varepsilon_{xx}^2 \end{matrix} \right\}, \tag{16a}$$

$$Q_{xz} = J_{66}\gamma_{xz}, \tag{16b}$$

with

$$\{A_{11},\ B_{11},\ D_{11},\ C_{11},\ F_{11},\ H_{11}\} = \int\limits_{-h/2}^{h/2} Q_{11}\Big\{1,\ z,\ z^2,\ f(z),\ zf(z),\ f(z)^2\Big\}\mathrm{d}z,$$

(17a)

$$J_{66} = \int\limits_{-h/2}^{h/2} Q_{66}\left[\frac{\mathrm{d}f(z)}{\mathrm{d}z}\right]^2 \mathrm{d}z.$$

(17b)

3.3 Strain energy

The strain energy functional of the FG beam is given by the following formula:

$$\delta U = \frac{1}{2}\int_V \big[\sigma_{xx}\varepsilon_{xx} + \tau_{xz}\gamma_{xz}\big]\mathrm{d}V.$$

(18)

Hence, we can rewrite the strain energy of the beam in the following form:

$$\delta U = \frac{1}{2}\int_A \left[N_{xx}\frac{\mathrm{d}\delta u}{\mathrm{d}x} + M_{xx}\frac{\mathrm{d}^2\delta w}{\mathrm{d}x^2} + P_{xx}\frac{\mathrm{d}\delta\varphi_x}{\mathrm{d}x} + Q_{xz}\delta\varphi_x\right]\mathrm{d}x\mathrm{d}z.$$

(19)

3.4 Kinetic energy

The kinetic energy of the beam at any instant can be expressed as follows:

$$T = \frac{1}{2}\int_A \rho(x,\ z)\left(\frac{\partial^2 u}{\partial t^2} + \frac{\partial^2 w}{\partial t^2}\right)\mathrm{d}x\mathrm{d}z.$$

(20)

3.5 Hamilton's principle

The kinematic hypotheses (displacement field) being defined for the geometry and the type of excitation studied, the vibrational approach systematically includes the following points:

(1) Calculation of deformations.
(2) Construction of the Hamilton functional.
(3) Externalization of the Hamilton functional.

In order to obtain the kinetic and strain energy, Hamilton's principle is written as

$$\int_{t_1}^{t_2} (\delta U - \delta T)\mathrm{d}t = 0.$$

(21)

3.6 Equations of motion

The appropriate equations of motion for displacement can be derived by using Hamilton's principle. By substituting Eqs. (19) and (20) into Eq. (21), we obtain

$$\frac{\partial N_{xx}}{\partial x} = I_0 \frac{\partial^2 u_0}{\partial t^2} - I_1 \frac{\partial^3 w_0}{\partial x \partial t^2} + I_3 \frac{\partial^2 \varphi_x}{\partial t^2}, \tag{22a}$$

$$\frac{\partial^2 M_{xx}}{\partial x^2} = I_0 \frac{\partial^2 w_0}{\partial t^2} + I_1 \frac{\partial^3 u_0}{\partial x \partial t^2} - I_2 \frac{\partial^4 w_0}{\partial x^2 \partial t^2} + I_4 \frac{\partial^3 \varphi_x}{\partial x \partial t^2}, \tag{22b}$$

$$\frac{\partial P_{xx}}{\partial x} - Q_{xz} = I_3 \frac{\partial^2 u_0}{\partial t^2} - I_4 \frac{\partial^3 w_0}{\partial x \partial t^2} + I_5 \frac{\partial^2 \varphi_x}{\partial t^2}, \tag{22c}$$

where the inertias are defined by

$$\{I_0, \, I_1, \, I_2, \, I_3, \, I_4, \, I_5\} = \int\limits_{-h/2}^{h/2} \rho(z) \Big\{ 1, \, z, \, z^2, \, f(z), \, zf(z), \, f(z)^2 \Big\} dz. \tag{23}$$

3.7 Nonlocal strain gradient theory

Lim et al. [34] introduced a stress function that incorporates both strain gradient stress and nonlocal elastic stress fields, which can be expressed as

$$\sigma_{ij} = \sigma_{ij}^{(0)} - \frac{d\sigma_{ij}^{(1)}}{dx}, \tag{24}$$

where $\sigma_{ij}^{(0)}$ represents the classical stress corresponding to strain ε_{kl}, and $\sigma_{ij}^{(1)}$ denotes the higher-order stress corresponding to strain gradient $\varepsilon_{kl,x}$. Additionally, their expressions can be described as follows:

$$\sigma_{ij}^{(0)} = \int_0^L C_{ijkl} \alpha_0 (x, \, x', \, e_0 a) \varepsilon_{kl,x} (x') dx', \tag{25a}$$

$$\sigma_{ij}^{(1)} = l^2 \int_0^L C_{ijkl} \alpha_1 (x, \, x', \, e_1 a) \varepsilon_{kl,x} (x') dx'. \tag{25b}$$

In this context, C_{ijkl} represents an elastic constant, and l is the material length scale parameter introduced to account for the influence of the strain gradient stress field. $e_0 a$ and $e_1 a$ are the nonlocal parameters introduced to consider the significance of the nonlocal elastic stress field. According to the nonlocal kernel functions $\alpha_0 (x, \, x', \, e_0 a)$ and

$\alpha_1(x, x', e_1a)$, the general constitutive relation for nonlocal strain can be expressed as per Eringen [4]:

$$\left[1 - (e_1a)^2\nabla^2\right]\left[1 - (e_0a)^2\nabla^2\right]\sigma_{ij} = C_{ijkl}\left[1 - (e_1a)^2\nabla^2\right]\varepsilon_{kl}$$
$$- C_{ijkl}l^2\left[1 - (e_0a)^2\nabla^2\right]\nabla^2\varepsilon_{kl}. \quad (26)$$

The symbol ∇^2 represents the Laplacian operator. In this study, we assume that $e = e_0 = e_1$. The complete nonlocal strain gradient constitutive relation can be formulated as follows:

$$\left[1 - \mu\nabla^2\right]\sigma_{ij} = C_{ijkl}\left[1 - \lambda\nabla^2\right]\varepsilon_{kl}, \quad (27)$$

where $\mu = (ea)^2$ and $\lambda = l^2$.

Hence, the constitutive relations for a nonlocal shear deformable functionally graded nanobeam can be represented as

$$\sigma_{xx} - \mu\frac{\partial^2\sigma_{xx}}{\partial x^2} = Q_{11}\left(\varepsilon_{xx} - \lambda\frac{\partial^2\varepsilon_{xx}}{\partial x^2}\right), \quad (28a)$$

$$\tau_{xz} - \mu\frac{\partial^2\sigma_{xx}}{\partial x^2} = Q_{66}\left(\gamma_{xz} - \lambda\frac{\partial^2\gamma_{xz}}{\partial x^2}\right). \quad (28b)$$

Thus, the equation governing stress resultants is

$$N_{xx} - \mu\frac{\partial^2 N_{xx}}{\partial x^2} = \left(1 - \lambda^2\frac{\partial^2}{\partial x^2}\right)\left[A_{11}\frac{\partial u_0}{\partial x} - B_{11}\frac{\partial^2 w_0}{\partial x^2} + C_{11}\frac{\partial\varphi_x}{\partial x}\right], \quad (29a)$$

$$M_{xx} - \mu\frac{\partial^2 M_{xx}}{\partial x^2} = \left(1 - \lambda^2\frac{\partial^2}{\partial x^2}\right)\left[B_{11}\frac{\partial u_0}{\partial x} - D_{11}\frac{\partial^2 w_0}{\partial x^2} + F_{11}\frac{\partial\varphi_x}{\partial x}\right], \quad (29b)$$

$$P_{xx} - \mu\frac{\partial^2 P_{xx}}{\partial x^2} = \left(1 - \lambda^2\frac{\partial^2}{\partial x^2}\right)\left[C_{11}\frac{\partial u_0}{\partial x} - F_{11}\frac{\partial^2 w_0}{\partial x^2} + H_{11}\frac{\partial\varphi_x}{\partial x}\right], \quad (29c)$$

$$Q_{xz} - \mu\frac{\partial^2 Q_{xz}}{\partial x^2} = \left(1 - \lambda\frac{\partial^2}{\partial x^2}\right)[J_{66}\varphi_x]. \quad (29d)$$

Substituting Eqs. (29) into Eqs. (22) to obtain

$$\left(1 - \lambda\nabla^2\right)\left(A_{11}\frac{\partial^2 u_0}{\partial x^2} - B_{11}\frac{\partial^3 w_0}{\partial x^3} + C_{11}\frac{\partial^2\varphi_x^1}{\partial x^2}\right)$$
$$- \left(1 - \mu\nabla^2\right)\left(I_0\frac{\partial^2 u_0}{\partial t^2} + I_1\frac{\partial^3 w_0}{\partial x\partial t^2} - I_3\frac{\partial^2\varphi_x}{\partial t^2}\right) = 0, \quad (30a)$$

$$\left(1 - \lambda \nabla^2\right) \left(B_{11} \frac{\partial^3 u_0}{\partial x^3} - D_{11} \frac{\partial^4 w_0}{\partial x^4} + F_{11} \frac{\partial^3 \varphi_x^1}{\partial x^3}\right)$$

$$- \left(1 - \mu \nabla^2\right) \left(I_0 \frac{\partial^2 w_0}{\partial t^2} - I_1 \frac{\partial^3 u_0}{\partial x \partial t^2} + I_2 \frac{\partial^4 w_0}{\partial x^2 \partial t^2} - I_4 \frac{\partial^3 \varphi_x}{\partial x \partial t^2}\right) = 0, \quad \text{(30b)}$$

$$\left(1 - \lambda \nabla^2\right) \left(C_{11} \frac{\partial^2 u_0}{\partial x^2} - F_{11} \frac{\partial^3 w_0}{\partial x^3} + H_{11} \frac{\partial^2 \varphi_x}{\partial x^2} - J_{66} \varphi_x\right)$$

$$- \left(1 - \mu \nabla^2\right) \left(-I_3 \frac{\partial^2 u_0}{\partial t^2} + I_4 \frac{\partial^3 w_0}{\partial x \partial t^2} - I_5 \frac{\partial^2 \varphi_x}{\partial t^2}\right) = 0. \quad \text{(30c)}$$

4 Analytical solution

The equations of motion are analytically solved for free vibration problems. Navier's solution method is used to determine the analytical solutions for a simply supported beam. We assume that the solution is of the following form:

$$u_0 = \sum_{m=1}^{\infty} U_m \cos(\beta x) e^{i\omega t}, \quad \text{(31a)}$$

$$w_0 = \sum_{m=1}^{\infty} W_m \sin(\beta x) e^{i\omega t}, \quad \text{(31b)}$$

$$\varphi_x = \sum_{m=1}^{\infty} X_m \cos(\beta x) e^{i\omega t}, \quad \text{(31c)}$$

where $\beta = m\pi/L$, and ω denotes the natural frequency, and U_m, W_m, X_m are arbitrary parameters. By replacing the Eqs. (31) in (30), the equations of motion become as follows:

$$\left([L] - \omega^2 [M]\right) \left\{ \begin{array}{c} U_m \\ W_m \\ X_m \end{array} \right\} = \left\{ \begin{array}{c} 0 \\ 0 \\ 0 \end{array} \right\}, \quad \text{(32)}$$

where the matrix $[L]$ and $[M]$ are the stiffness and mass matrix, respectively

$$[L] = \left(1 + \lambda \beta^2\right) \begin{bmatrix} L_{11} & L_{12} & L_{13} \\ L_{12} & L_{22} & L_{23} \\ L_{13} & L_{23} & L_{33} \end{bmatrix}, \quad \text{(33a)}$$

$$[M] = \left(1 + \mu\beta^2\right) \begin{bmatrix} M_{11} & M_{12} & M_{13} \\ M_{12} & M_{22} & M_{23} \\ M_{13} & M_{23} & M_{33} \end{bmatrix}, \tag{33b}$$

with

$$
\begin{aligned}
&L_{11} = -A_{11}\beta^2, \quad L_{12} = B_{11}\beta^3, \quad L_{13} = -C_{11}\beta^2, \\
&L_{22} = -D_{11}\beta^4, \quad L_{23} = F_{11}\beta^3, \quad L_{33} = -\left(H_{11}\beta^2 + J_{66}\right),
\end{aligned}
\tag{34}
$$

and

$$
\begin{aligned}
&M_{11} = -I_0, \quad M_{12} = I_1\beta, \\
&M_{13} = -I_3, \\
&M_{22} = -I_0 - I_2\beta^2, \quad M_{23} = I_4\beta, \quad M_{33} = -I_5.
\end{aligned}
\tag{35}
$$

For the classical theory (CPT),

$$L_{13} = L_{23} = L_{33} = 0 \quad \text{and} \quad M_{13} = M_{23} = M_{33} = 0. \tag{36}$$

5 Numerical results

In this section, several numerical examples are presented and discussed in detail to demonstrate the influences of various parameters, such as nonlocal parameters, length scale parameters, length-to-thickness ratio, and power-law index, on the free vibration response of FG nanobeams. The analyzed FG beam is made of a mixture of metal (Aluminum, Al) and ceramic (Alumina-Al_2O_3). The material properties of both Aluminum and Alumina are given as follows:

$$\text{Aluminum Al: } E_m = 70\,\text{GPa}, \quad \rho_m = 2702\,\text{kg/m}^3, \quad \upsilon_m = 0.3,$$

$$\text{Alumina Al}_2\text{O}_3\text{: } E_c = 3960\,\text{GPa}, \quad \rho_c = 3800\,\text{kg/m}^3, \quad \upsilon_m = 0.3.$$

The non-dimensional functions of deflection, axial stress, shear stress, and transverse stress are defined by

$$\overline{\omega} = \omega \frac{L^2}{h} \sqrt{\frac{\rho_m}{E_m}}. \tag{37}$$

Table 1 Comparison of the non-dimensional fundamental natural frequency of FG beams with various boundary conditions ($L/h = 5$)

Sources	p					
	0	0.5	1	2	5	10
Thai et al. [1] (TBT)	5.1527	4.4107	3.9904	3.6264	3.4012	3.2816
SBT [1]	5.1531	4.4110	3.9907	3.6263	3.3998	3.2811
Simsek [2] (TBT)	5.1527	4.4111	3.9904	3.6264	3.4012	3.2816
Simsek [2] (SBT)	5.1531	4.4114	3.9907	3.6263	3.3998	3.2811
Vo et al. [3] (TBT)	5.1528	4.4019	3.9716	3.5979	3.3743	3.2653
Nguyen et al. [4] (HBT)	5.1528	4.4019	3.9716	3.5979	3.3743	3.2653
Present	5.1527	4.4107	3.9904	3.6264	3.4012	3.2816

5.1 Comparison study

To validate the accuracy and effectiveness of the suggested model for predicting the free vibration characteristics of FG beams, the numerical outcomes are cross-referenced with previously published findings. Table 1 illustrates the comparison between the current results and those from studies by Thai and Vo [40], Şimşek [41], Vo et al. [42], and Nguyen et al. [39]. The theories utilized encompass the third-order shear deformation theory (TBT), the sinusoidal shear deformation theory (SBT), and the hyperbolic shear deformation theory (HBT). In this comparison, the volume fraction varies across the transverse direction according to the function $(1/2 + z/h)^p$. It is evident that the disparities between the current findings and the cited literature are negligible. Hence, the proposed model demonstrates precision, resilience, and efficiency in analyzing the current model.

5.2 Parametric study

5.2.1 Effect of power-law indexes

Table 2 presents the effect of power-law indexes p and k on the dimensionless frequencies of various schemes of FG beams. Additionally, Fig. 4 describes the effect of power-law index p on the dimensionless frequencies of various schemes of bi-coated beams ($k = 2$, $L/h = 10$, $\mu = \lambda = 0$). Firstly, both types of FG-C beams, hardcore beams and softcore beams, are ignored in the plot because they are independent of "p." The increase in index p leads to an augmentation of the proportion of ceramic in FG-A hardcore beams and a reduction of the proportion of ceramic in FG-A softcore (SC) beams; therefore, the dimensionless frequency increases for FG-A hardcore beams and decreases for FG-A softcore (SC) beams.

The effect of power-law index k on the dimensionless frequencies of various schemes of FG beams ($p = 2$, $L/h = 10$, $\mu = \lambda = 0$) is plotted in Fig. 5. As

Table 2 Effect of power-law indexes p and k on the dimensionless frequencies of various schemes of FG beams ($L/h = 10$, $\mu = \lambda = 0$)

p	k	HC-FGM			SC-FGM		
		FG-A	FG-B	FG-C	FG-A	FG-B	FG-C
2	2	3.7836	2.9848	4.7152	5.1211	5.6573	6.0876
	6	3.9711	2.9848	6.0446	5.0149	5.6573	6.2329
	8	3.9998	2.9848	6.2723	4.9951	5.6573	6.2555
	10	4.0178	2.9848	6.4189	4.9820	5.6573	6.2696
6	2	4.3017	5.0688	4.7152	4.7417	5.9505	6.0876
	6	4.5575	5.0688	6.0446	4.4689	5.9505	6.2329
	8	4.5961	5.0688	6.2723	4.4172	5.9505	6.2555
	10	4.6201	5.0688	6.4189	4.3831	5.9505	6.2696
8	2	4.4102	5.4698	4.7152	4.6395	6.0195	6.0876
	6	4.6793	5.4698	6.0446	4.3172	6.0195	6.2329
	8	4.7197	5.4698	6.2723	4.2557	6.0195	6.2555
	10	4.7449	5.4698	6.4189	4.2152	6.0195	6.2696
10	2	4.4837	5.7375	4.7152	4.5653	6.0674	6.0876
	6	4.7615	5.7375	6.0446	4.2053	6.0674	6.2329
	8	4.8032	5.7375	6.2723	4.1363	6.0674	6.2555
	10	4.8291	5.7375	6.4189	4.0907	6.0674	6.2696

the previous analysis, the FG-B beams are ignored in the plot because they are independent of "k." From this figure, the increase in index k leads to an increase in the proportion of ceramic in FG-A hardcore beams and a decrease in the proportion of ceramic in FG-A softcore beams. As a result, the dimensionless frequency increases for FG-A hardcore beams and decreases for FG-A softcore (SC) beams.

5.2.2 Effect of the thickness ratio

Table 3 illustrates the effect of the thickness ratio L/h on the dimensionless frequencies of various schemes of FG beams. The graphs in Fig. 6 show the effect of the thickness ratio L/h on the dimensionless frequencies of various schemes of FG beams ($p = k = 5$, $\mu = \lambda = 0$). From this figure, it is apparent that as the thickness ratio L/h increases, the dimensionless frequencies increase across all types of beams. Furthermore, beyond $L/h > 15$, the dimensionless frequencies remain nearly constant irrespective of the beam type. Thus, it can be inferred that the maximum dimensionless frequencies are achieved for FG-C softcore beams.

5.2.3 Effect of the nonlocal and the length scale parameters

The size-dependent effects represented by the nonlocal and length scale parameters are tabulated in Table 4. Figure 7 describes the effect of the nonlocal parameter μ on the
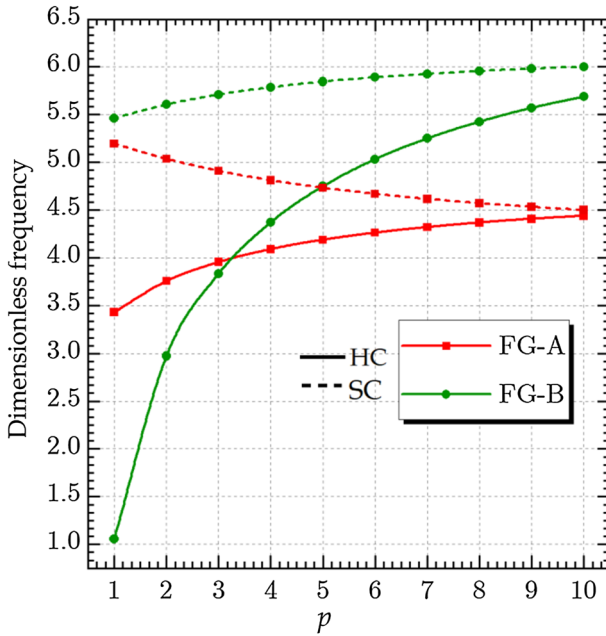
Fig. 4 Effect of power-law indexes p on the dimensionless frequencies of various schemes of FG beams ($k = 2$, $L/h = 10$, $\mu = \lambda = 0$)
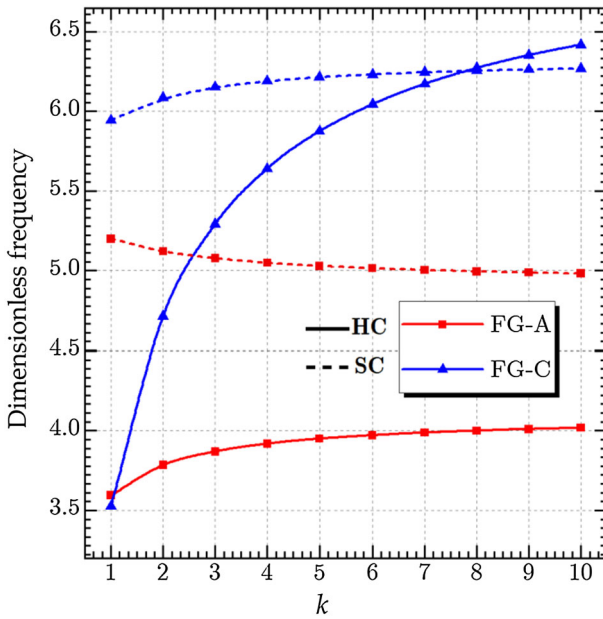

Fig. 5 Effect of power-law index k on the dimensionless frequencies of various schemes of FG beams ($p = 2$, $L/h = 10$, $\mu = \lambda = 0$)

Table 3 Effect of the thickness ratio L/h on the dimensionless frequencies of various schemes of FG beams ($\mu = \lambda = 0$)

$p = k$	L/h	HC-FGM			SC-FGM		
		FG-A	FG-B	FG-C	FG-A	FG-B	FG-C
2	5	3.6564	2.9047	4.5049	4.8286	5.4419	5.8161
	10	3.7836	2.9848	4.7152	5.1211	5.6573	6.0876
	15	3.8091	3.0006	4.7583	5.1827	5.7009	6.1433
	30	3.8247	3.0102	4.7849	5.2209	5.7276	6.1776
6	5	4.3847	4.8866	5.7750	4.1949	5.7083	5.9549
	10	4.5575	5.0688	6.0446	4.4689	5.9505	6.2329
	15	4.5925	5.1054	6.0999	4.5271	5.9998	6.2899
	30	4.6139	5.1279	6.1340	4.5634	6.0301	6.3251
8	5	4.5349	5.2633	5.9926	3.9987	5.7701	5.9765
	10	4.7197	5.4698	6.2723	4.2557	6.0195	6.2555
	15	4.7571	5.5115	6.3297	4.3102	6.0703	6.3127
	30	4.7801	5.5371	6.3651	4.3442	6.1015	6.3480
10	5	4.6359	5.5141	6.1326	3.8484	5.8129	5.9900
	10	4.8291	5.7375	6.4189	4.0907	6.0674	6.2696
	15	4.8683	5.7828	6.4776	4.1420	6.1192	6.3270
	30	4.8924	5.8106	6.5138	4.1739	6.1512	6.3623

dimensionless frequencies of various schemes of FG beams ($p = k = 1$, $L/h = 10$). As observed, an increase in the nonlocal parameter μ leads to a permanent decrease in the beam stiffness and consequently the dimensionless frequencies across all beam types. Conversely, it can be inferred that the minimum frequencies are attained for hardcore FG beams.

Figure 8 illustrates the effect of the length scale parameter λ on the dimensionless frequencies of various schemes of FG beams ($p = k = 1$, $L/h = 10$). It is crucial to note that as the length scale parameter λ increases, the dimensionless frequencies of different schemes of FG beams increase significantly. This can be attributed to the enhancement in beam stiffness. Additionally, it is noteworthy that the frequencies of hardcore FG beams are lower than those of softcore FG beams.

6 Conclusion

This study investigates the inherent vibrational characteristics of an innovative functionally graded nanobeam. Specifically, we explore two prevalent types of functionally graded material (FGM) structures: hardcore FGM and softcore FGM, each comprising three distinct configurations. The FGM nanobeam under consideration has material
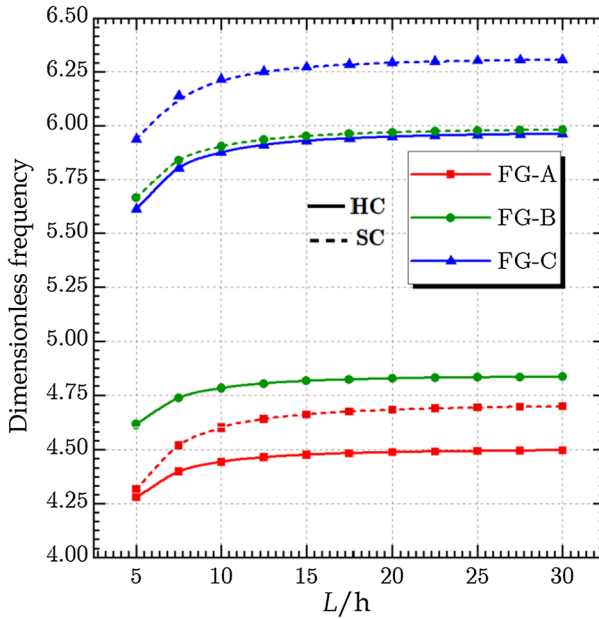
Fig. 6 Effect of the thickness ratio L/h on the dimensionless frequencies of various schemes of FG beams ($p = k = 5$, $\mu = \lambda = 0$)

properties that continuously change in both longitudinal and transverse directions, following a composite power-law distribution based on constituent volume fractions. We employ a novel higher-order shear deformation plate theory to establish the governing equations for the FGM beam, with the beam subjected to simply supported boundary conditions. Additionally, we incorporate the nonlocal strain gradient theory to account for microstructure-dependent effects. Based on the numerical results, several conclusions can be drawn. Firstly, the choice of beam schemes, whether hardcore or softcore, and the specific distribution patterns of materials (FG-A, FG-B, and FG-C) significantly influence the stiffness of the beam, thereby affecting the fundamental frequencies of the system. Furthermore, the data clearly illustrate that an increase in the nonlocal parameter reduces beam stiffness, and decreasing the length scale parameter also results in decreased stiffness [43–50].

Table 4 Effect of the nonlocal parameter μ and the length scale parameter λ on the dimensionless frequencies of various schemes of bi-coated beams ($p = k = 1$, $L/h = 10$)

| μ	λ	HC-FGM			SC-FGM		
		FG-A	FG-B	FG-C	FG-A	FG-B	FG-C
0	0	3.3207	1.0573	3.5255	5.3113	5.5128	5.9447
	0.5	3.4016	1.0830	3.6114	5.4408	5.6472	6.0896
	1	3.4807	1.1082	3.6954	5.5672	5.7784	6.2311
	1.5	3.5580	1.1328	3.7775	5.6909	5.9068	6.3695
	2	3.6336	1.1569	3.8578	5.8119	6.0324	6.5050
0.5	0	3.2416	1.0321	3.4416	5.1849	5.3816	5.8032
	0.5	3.3207	1.0573	3.5255	5.3113	5.5128	5.9447
	1	3.3978	1.0818	3.6074	5.4348	5.6409	6.0829
	1.5	3.4733	1.1059	3.6876	5.5555	5.7662	6.2180
	2	3.5472	1.1294	3.7660	5.6736	5.8888	6.3502
1	0	3.1680	1.0087	3.3634	5.0671	5.2594	5.6714
	0.5	3.2452	1.0333	3.4454	5.1907	5.3876	5.8096
	1	3.3207	1.0573	3.5255	5.3113	5.5128	5.9447
	1.5	3.3944	1.0808	3.6038	5.4293	5.6352	6.0767
	2	3.4666	1.1037	3.6804	5.5447	5.7551	6.2060
1.5	0	3.0992	0.9868	3.2903	4.9570	5.1451	5.5482
	0.5	3.1747	1.0108	3.3706	5.0779	5.2705	5.6834
	1	3.2485	1.0343	3.4489	5.1959	5.3930	5.8155
	1.5	3.3207	1.0573	3.5255	5.3113	5.5128	5.9447
	2	3.3913	1.0798	3.6005	5.4243	5.6300	6.0711
2	0	3.0346	0.9662	3.2218	4.8538	5.0379	5.4326
	0.5	3.1086	0.9898	3.3004	4.9721	5.1608	5.5651
	1	3.1809	1.0128	3.3771	5.0877	5.2807	5.6944
	1.5	3.2515	1.0353	3.4521	5.2007	5.3980	5.8209
	2	3.3207	1.0573	3.5255	5.3113	5.5128	5.9447
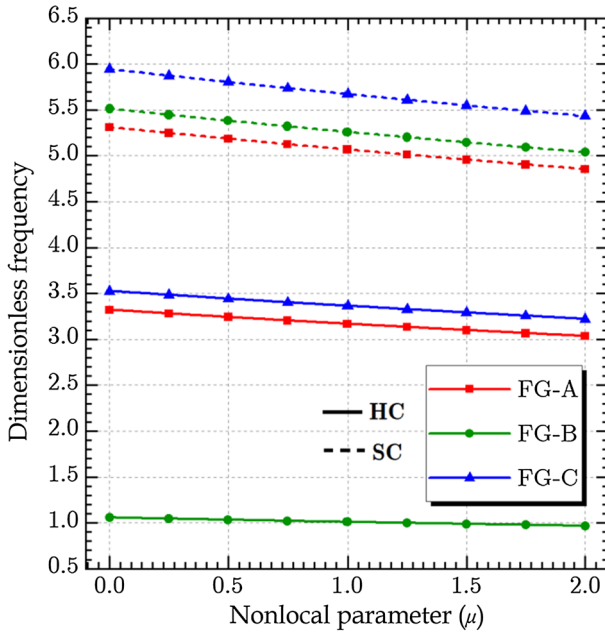
Fig. 7 Effect of the nonlocal parameter μ on the dimensionless frequencies of various schemes of bi-coated beams ($p = k = 1$, $L/h = 10$)
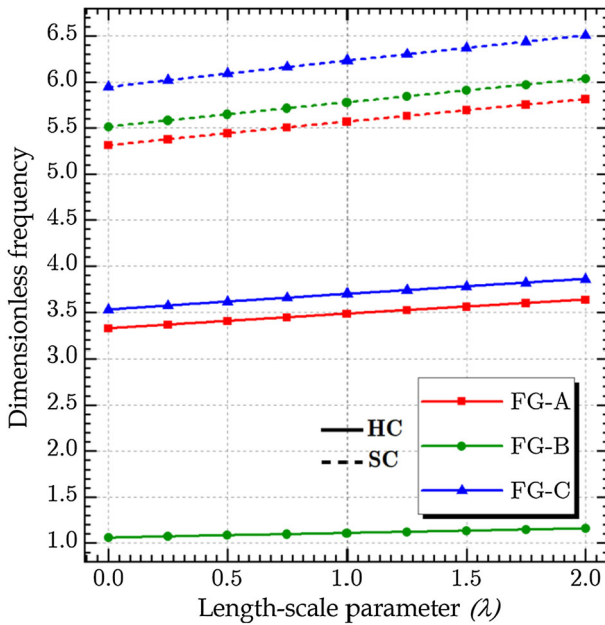

Fig. 8 Effect of the length scale parameter λ on the dimensionless frequencies of various schemes of bi-coated beams ($p = k = 1$, $L/h = 10$)

Author contributions MG contributed toward data curation, formal analysis, methodology, resources, validation, funding acquisition, and writing draft version; AD contributed toward methodology, investigation, formal analysis, data curation, and conceptualization; AAD contributed toward investigation, methodology, software, validation, visualization, supervision, and writing—original draft; MSAH contributed toward conceptualization, methodology, and writing—review and editing; BA contributed toward software and writing—review and editing; MAE contributed toward methodology and writing—review and editing; and M-OB contributed toward data curation, formal analysis, writing—review and editing, and conceptualization.

Declarations

Conflict of interest The authors declare that they have no conflict of interest.

References

1. Ekinci K, Roukes M (2005) Nanoelectromechanical systems. Rev Sci Instrum 76(6):061101
2. Rahmani O, Refaeinejad V, Hosseini S (2017) Assessment of various nonlocal higher order theories for the bending and buckling behavior of functionally graded nanobeams. Steel Compos Struct 23(3):339–350
3. Eringen AC (1972) Nonlocal polar elastic continua. Int J Eng Sci 10:1–16
4. Eringen AC (1983) On differential equations of nonlocal elasticity and solutions of screw dislocation and surface waves. J Appl Phys 54(9):4703–4710
5. Bezzina S, Bessaim A, Houari MSA, Azab M (2022) A new quasi-3D plate theory for free vibration analysis of advanced composite nanoplates. Steel Compos Struct 45(6):839–850
6. Peng W, Chen L, He T (2021) Nonlocal thermoelastic analysis of a functionally graded material microbeam. Appl Math Mech 42(6):855–870
7. Ceballes S, Larkin K, Rojas E, Ghaffari SS, Abdelkefi A (2021) Nonlocal elasticity and boundary condition paradoxes: a review. J Nanopart Res 23:1–27
8. Eltaher M, Khater M, Emam SA (2016) A review on nonlocal elastic models for bending, buckling, vibrations, and wave propagation of nanoscale beams. Appl Math Model 40(5–6):4109–4128
9. Farajpour A, Ghayesh MH, Farokhi H (2018) A review on the mechanics of nanostructures. Int J Eng Sci 133:231–263
10. Peddieson J, Buchanan GR, McNitt RP (2003) Application of nonlocal continuum models to nanotechnology. Int J Eng Sci 41(3–5):305–312
11. Ebrahimi F, Salari E (2015b) Nonlocal thermo-mechanical vibration analysis of functionally graded nanobeams in thermal environment. Acta Astronaut 113:29–50
12. Xu X-J, Deng Z-C, Zhang K, Meng J-M (2016) Surface effects on the bending, buckling and free vibration analysis of magneto-electro-elastic beams. Acta Mech 227:1557–1573
13. Fang J, Zheng S, Xiao J, Zhang X (2020) Vibration and thermal buckling analysis of rotating nonlocal functionally graded nanobeams in thermal environment. Aerosp Sci Technol 106:106146
14. Reddy J (2007) Nonlocal theories for bending, buckling and vibration of beams. Int J Eng Sci 45(2–8):288–307
15. Wang Q, Liew K (2007) Application of nonlocal continuum mechanics to static analysis of micro- and nano-structures. Phys Lett A 363(3):236–242
16. Borjalilou V, Taati E, Ahmadian MT (2019) Bending, buckling and free vibration of nonlocal FG-carbon nanotube-reinforced composite nanobeams: exact solutions. SN Appl Sci 1:1–15
17. Yin G-S, Deng Q-T, Yang Z-C (2015) Bending and buckling of functionally graded Poisson's ratio nanoscale beam based on nonlocal theory. Iran J Sci Technol (Sci) 39(4):559–565
18. Ebrahimi F, Barati MR (2016) Vibration analysis of nonlocal beams made of functionally graded material in thermal environment. Eur Phys J Plus 131:1–22
19. Barretta R, de Sciarra FM (2018) Constitutive boundary conditions for nonlocal strain gradient elastic nano-beams. Int J Eng Sci 130:187–198
20. Romano G, Barretta R (2017a) Stress-driven versus strain-driven nonlocal integral model for elastic nano-beams. Composites B 114:184–188

21. Challamel N, Mechab I, Elmeiche N, Houari MSA, Ameur M, Ait Atmane A (2013) Buckling of generic higher-order shear beam/columns with elastic connections: local and nonlocal formulation. J Eng Mech 139(8):1091–1109

22. Li C, Yao L, Chen W, Li S (2015) Comments on nonlocal effects in nano-cantilever beams. Int J Eng Sci 87:47–57

23. Apuzzo A, Barretta R, Luciano R, de Sciarra FM, Penna R (2017) Free vibrations of Bernoulli-Euler nano-beams by the stress-driven nonlocal integral model. Composites B 123:105–111

24. Lovisi G (2023) Application of the surface stress-driven nonlocal theory of elasticity for the study of the bending response of FG cracked nanobeams. Compos Struct 324(1):117549

25. Penna R (2023) Bending analysis of functionally graded nanobeams based on stress-driven nonlocal model incorporating surface energy effects. Int J Eng Sci 189:103887

26. Romano G, Barretta R (2017b) Nonlocal elasticity in nanobeams: the stress-driven integral model. Int J Eng Sci 115:14–27

27. Yang F, Chong A, Lam DCC, Tong P (2002) Couple stress based strain gradient theory for elasticity. Int J Solids Struct 39(10):2731–2743

28. Akgöz B, Civalek O (2014) Thermo-mechanical buckling behavior of functionally graded microbeams embedded in elastic medium. Int J Eng Sci 85:90–104

29. Ansari R, Gholami R, Shojaei MF, Mohammadi V, Sahmani S (2013) Size-dependent bending, buckling and free vibration of functionally graded Timoshenko microbeams based on the most general strain gradient theory. Compos Struct 100:385–397

30. Ma H, Gao XL, Reddy J (2008) A microstructure-dependent Timoshenko beam model based on a modified couple stress theory. J Mech Phys Solids 56(12):3379–3391

31. Li X, Li L, Hu Y, Ding Z, Deng W (2017) Bending, buckling and vibration of axially functionally graded beams based on nonlocal strain gradient theory. Compos Struct 165:250–265

32. Şimşek M, Reddy J (2013) Bending and vibration of functionally graded microbeams using a new higher order beam theory and the modified couple stress theory. Int J Eng Sci 64:37–53

33. Papargyri-Beskou S, Tsepoura K, Polyzos D, Beskos D (2003) Bending and stability analysis of gradient elastic beams. Int J Solids Struct 40(2):385–400

34. Lim C, Zhang G, Reddy J (2015) A higher-order nonlocal elasticity and strain gradient theory and its applications in wave propagation. J Mech Phys Solids 78:298–313

35. Li L, Hu Y, Ling L (2016) Wave propagation in viscoelastic single-walled carbon nanotubes with surface effect under magnetic field based on nonlocal strain gradient theory. Physica E 75:118–124. ISSN 1386-9477

36. Li L, Li X, Hu Y (2016) Free vibration analysis of nonlocal strain gradient beams made of functionally graded material. Int J Eng Sci 102:77–92

37. Özmen R, Kılıç R, Esen I (2024) Thermomechanical vibration and buckling response of nonlocal strain gradient porous FG nanobeams subjected to magnetic and thermal fields. Mech Adv Mater Struct 31(4):834–853

38. Daikh AA, Houari MSA, Belarbi MO, Chakraverty S, Eltaher MA (2022) Analysis of axially temperature-dependent functionally graded carbon nanotube reinforced composite plates. Eng Comput 38(Suppl 3):2533–2554

39. Nguyen T-K, Truong-Phong Nguyen T, Vo TP, Thai H-T (2015) Vibration and buckling analysis of functionally graded sandwich beams by a new higher-order shear deformation theory. Composites B 76:273–285

40. Thai HT, Vo PT (2012) Bending and free vibration analysis of functionally graded beams employing different higher-order shear deformation beam theories. Int J Mech Sci 62:57–66

41. Şimşek M (2010) Fundamental frequency analysis of functionally graded beams employing various higher-order beam theories. Nucl Eng Des 240(4):697–705

42. Vo TP, Thai H-T, Nguyen T-K, Maheri A, Lee J (2014) Finite element model for vibration and buckling analysis of functionally graded sandwich beams using a refined shear deformation theory. Eng Struct 64:12–22

43. Askes H, Aifantis EC (2009) Gradient elasticity and flexural wave dispersion in carbon nanotubes. Phys Rev B 80(19):195412

44. Babaei Gavan K, Westra HJ, van der Drift EW, Venstra WJ, van der Zant HS (2009) Size-dependent effective Young's modulus of silicon nitride cantilevers. Appl Phys Lett 94(23):233108

45. Ebrahimi F, Salari E (2015a) Thermal buckling and free vibration analysis of size-dependent Timoshenko FG nanobeams in thermal environments. Compos Struct 128:363–380. ISSN 0263-8223

46. Eringen AC, Edelen DGB (1972) On nonlocal elasticity. Int J Eng Sci 10:233–248
47. Garg A, Chalak HD, Zenkour AM, Belarbi MO, Houari MSA (2021) A review of available theories and methodologies for the analysis of nano isotropic, nano functionally graded, and CNT reinforced nanocomposite structures. Arch Comput Methods Eng 29:1–34
48. Li L, Hu Y (2016) Nonlinear bending and free vibration analyses of nonlocal strain gradient beams made of functionally graded material. Int J Eng Sci 107:77–97
49. Romano G, Barretta R, Diaco M, de Sciarra FM (2017) Constitutive boundary conditions and paradoxes in nonlocal elastic nanobeams. Int J Mech Sci 121:151–156
50. Touloukian TS (1967) Thermophysical properties of high temperature solid materials. In: Elements. Macmillan, New York, p 1